Voltage-Probe-Position Dependence and Magnetic-Flux Contribution to the Measured Voltage in ac Transport Measurements: Which Measuring Circuit Determines the Real Losses?

Thomas Pe, Jason McDonald, and John R. Clem

Ames Laboratory-USDOE and Department of Physics and Astronomy,
Iowa State University, Ames, IA

Abstract: The voltage V_{ab} measured between two voltage taps a and b during magnetic flux transport in a type-II superconductor carrying current I is the sum of two contributions, the line integral from a to b of the electric field along an arbitrary path C_s through the superconductor and a term proportional to the time rate of change of magnetic flux through the area bounded by the path C_s and the measuring circuit leads. When the current $I(t)$ is oscillating with time t, the apparent ac loss (the time average of the product IV_{ab}) depends upon the measuring circuit used. Only when the measuring-circuit leads are brought out far from the surface does the apparent power dissipation approach the real (or true) ac loss associated with the length of sample probed. Calculations showing comparisons between the apparent and real ac losses in a flat strip of rectangular cross section will be presented, showing the behavior as a function of the measuring-circuit dimensions. Corresponding calculations also are presented for a sample of elliptical cross section.

1 Introduction

As high-temperature superconducting materials move closer to large-scale electric-power applications, it is increasingly important to understand the magnitude and origin of the ac losses in these materials. Ideally, measurements of such losses should be carried out under experimental conditions close to those of the proposed applications. For example, for testing materials intended for use in ac power transmission cables, it is preferable that the ac losses be measured while the conductor is carrying an applied ac transport current.

To be published in the *Proceedings of the First Polish-U.S. Conference on High Temperature Superconductivity*, Wroclaw and Duszniki-Zdroj, September 11-15, 1995, by Springer-Verlag in their series "Lecture Notes in Physics."

In measuring the low-frequency ac losses of normal metals, it is safe to use the simple procedure of (a) applying an ac current $I(t) = I_0 \cos\omega t$, (b) using a high-impedance voltmeter to measure the corresponding voltage $V(t)$ between a pair of voltage taps across a representative segment of the conductor, and (c) obtaining the average rate of power dissipation from $P = \langle I(t)V(t)\rangle$, where the brackets denote the time average. It is at first surprising to learn that when the sample is a type-II superconducting tape or strip, this simple method runs into serious difficulties: The apparent rate of power dissipation $P_{\rm app}$ so obtained depends on where the voltage taps are placed on the tape (along an edge or along the centerline) and on how far away from the tape the voltage leads are extended before they are brought together, twisted, and led out to the voltmeter ([1],[2],[3]).

As emphasized by Campbell ([4]), to explain these results it is important to account for the fact that when low-resistance leads are attached at contact points a and b on the conductor, the time-dependent voltage $V_{\rm ab}$ measured by a high-impedance voltmeter is the sum of an electric-field integral term and a magnetic-flux term. As shown in Refs. ([5][6][7]), this voltage is

$$V_{\rm ab} = \int_a^b \boldsymbol{E}\cdot d\boldsymbol{l} - \frac{d}{dt}\Phi_{\rm sm} \quad , \tag{1}$$

where the line integral is to be carried out from a to b along a path $C_{\rm s}$ through the conductor, and $\Phi_{\rm sm}$ is the magnetic flux up through the loop bounded by the path $C_{\rm s}$ and the measuring circuit leads (which define the contour $C_{\rm m}$). It can be shown with the help of Faraday's law that the voltage $V_{\rm ab}$ is independent of the contour $C_{\rm s}$, because any change in the first term on the right-hand side of Eq. (1) is compensated by a canceling change in the second term. It often is convenient to chose the contour $C_{\rm s}$ so that the first term is zero.

Because of magnetic hysteresis, the flux term, i.e., the second term on the right-hand side of Eq. (1), has terms in strip geometry that are both in phase and out of phase with the current $I(t)$. Only for normal-metal wires in which the current density is uniform and for superconducting wires that have circular cross section does the contribution to the flux term from magnetic fields outside the sample have a vanishing in-phase component. As pointed out by Campbell ([4]), in general only when the leads are brought out to a large distance before bringing them together does the measurement give the true loss, i.e., the dissipated power delivered by the power supply to the segment between a and b. Since the true loss involves the voltage measured across the terminals of the power supply, the flux $\Phi_{\rm sm}$ involved in Eq. (1) is the total flux through the area bounded by the contour $C_{\rm s}$ along the the sample of interest and the contour $C_{\rm m}$ along the leads that connect the sample to the power supply.

In Sec. 2, we present the details of how to calculate the measured time-dependent voltage $V(t)$ generated by hysteretic losses in a flat strip of rectangular cross section carrying an alternating current $I(t)$. We show how the apparent loss depends upon the measuring circuit geometry and examine the conditions under which the apparent loss is a good approximation to the true loss. We also

present the corresponding results for a sample of elliptical cross section. In Sec. 3, we briefly summarize our results.

2 Theoretical Approach and Results

Consider a type-II superconducting strip of width $2W$ and thickness $d \ll 2W$ in the xy plane, centered on the y axis, as shown in Fig. 1, such that the edges are at $x = \pm W$. Assume that the London penetration depth λ is less than the sample thickness. Suppose that an alternating current $I_y(t) = I_0 \cos \omega t$ is applied. A corresponding self-field, which wraps around the sample, will be produced. If the current amplitude is very tiny, the magnitude of the field at the sample edges will be less than the lower critical field H_{c1} and thus will be too small to cause any vortices to penetrate into the sample. However, we are most interested in the case for which the current amplitude I_0 is substantial, such that vortices or antivortices are nucleated at the edges and driven into the sample during each half cycle.

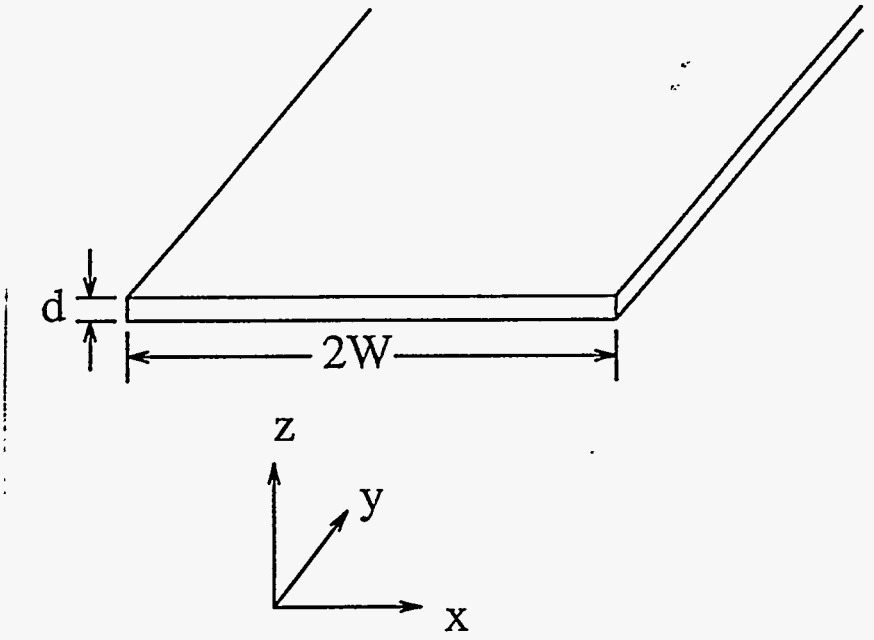

Fig. 1. Sketch of strip geometry considered in this paper. The properties of long current-carrying type-II superconductors of width $2W$ and thickness $d \ll 2W$ are examined.

To calculate the hysteretic losses under such circumstances, we use the critical state model, which is characterized by a critical depinning current density J_c.

We assume for simplicity in this paper that J_c is independent of the flux density B. We also assume that over most of the vortex-filled region, the local field is sufficiently large by comparison with H_{c1} that we may take $B = \mu_0 H$ to good approximation. At each value of the current $I_y(t)$ (assuming that the current amplitude I_0 is less than the critical current $I_c = 2WdJ_c$), the quasistatic profiles of the current density $J_y(x,t)$ (averaged across the sample thickness) and the magnetic flux density $B(x,z,t)$ may be calculated using the Norris method [8] as described in detail in Refs. [9] and [10].

When the current $I_y(t)$ is equal to I_0, magnetic flux penetrates from both edges to the coordinates $x = \pm a_0$, where $a_0 = W\sqrt{1-(I_0/I_c)^2}$, but $B_z(x,0,t)$ remains zero in the unpenetrated region $|x| < a_0$. The current density J_y in the strip is given by

$$J_y(x;a_0) = \begin{cases} \frac{2}{\pi} J_c \arctan\sqrt{\frac{W^2-a_0^2}{a_0^2-x^2}}, & |x| < a_0, \\ J_c, & a_0 < |x| < W. \end{cases} \tag{2}$$

As $I_y(t)$ decreases, however, new flux fronts move in from both edges. The current density in each of these new regions has magnitude J_c, but it is reversed in direction. Let $x = \pm a(t)$ denote the time-dependent coordinates of these incoming flux fronts. As shown in Refs. [9] and [10], the current density in the strip can be expressed as the superposition of two distributions,

$$J_y(x,t) = J_y(x;a_0) - 2J_y(x;a), \tag{3}$$

where the function $J_y(x;a)$ is defined in Eq. (2), $a(t) = W\sqrt{1-(I_a/I_c)^2}$, and $I_a = [I_0 - I_y(t)]/2$. Note that $a(t) = W$ when $I_y(t) = I_0$, and $a(t) = a_0$ when $I_y(t) = -I_0$.

From the Biot-Savart law, it follows that the magnetic flux density $B(x,z,t)$ in the vicinity of the strip also can be written as the superposition of two fields,

$$B(x,z,t) = B(x,z;a_0) - 2B(x,z;a), \tag{4}$$

where $B(x,z;a_0)$ is the magnetic flux density generated by the current density given in Eq. (2). Of the two terms on the right-hand side of Eq. (4), the first is independent of t, while the second one depends upon t via the coordinate $a(t)$.

Having briefly discussed how to calculate the time-dependent magnetic flux density in the strip, we now turn to the problem of calculating the apparent and real rates of power dissipation. It is well known that the rate of power dissipation for hysteretic losses is linear in frequency, since there is a fixed amount of energy dissipated each cycle. We thus calculate the apparent and real loss per cycle per unit length of the strip. For simplicity, we consider two special circuit configurations:

Perpendicular case (Fig. 2). Here the voltage taps are placed along the centerline of the strip ($x = 0, z = d/2$), and the leads extend perpendicular to the surface to a height z before they are brought together, twisted, and led out to the voltmeter.

Parallel case (Fig. 3). Here the voltage taps are placed along the edge of the strip ($x = W, z = 0$), and the leads lie in the plane of the strip but extend perpendicular to the edge to the coordinate $x > W$ before they are brought together, twisted, and led out to the voltmeter.

The measured voltage for both cases is determined by Eq. (1), where the contours C_s extend along the line $x = z = 0$ except for segments that extend perpendicular to this line out to the voltage taps, as shown by the dotted lines in Figs. 2 and 3. It can be shown that the line integrals of the electric field [the first term of Eq. (1)] vanish for these choices of C_s. To calculate the voltage $V_{ab}(t)$ for these cases, we therefore need only to calculate the time derivative of the magnetic flux through the shaded areas in the measuring circuits sketched in Figs. 2 and 3. The time derivative of the magnetic flux is obtained by first using the Biot-Savart law to express the magnetic field in terms of $J_y(x,t)$, as sketched in Eq. (4), and by taking the time derivative of the resulting expression using Eq. (3) and the connection between $a(t)$ and $I_y(t)$. The apparent loss per cycle per unit length is then obtained by evaluating $\int I_y(t)V_{ab}(t)\,dt$ over one period $(2\pi/\omega)$, where $V_{ab}(t)$ is the voltage across unit length of the sample.

The apparent loss per cycle per unit length for the strip in the perpendicular case is

$$
\begin{aligned}
L_\perp(F) = \left(\frac{\mu_0 I_c^2}{\pi}\right) \times
&\left[2\left(\frac{z}{W}\right)\left(\sqrt{\left(\frac{z}{W}\right)^2+1}-\sqrt{\left(\frac{z}{W}\right)^2+1-F^2}\right.\right.\\
&\left.\left.- F\arctan\left(\frac{F}{\sqrt{\left(\frac{z}{W}\right)^2+1-F^2}}\right)\right)\right.\\
&- \frac{F^2}{2}\log\left(\frac{\sqrt{1-F^2}\left(\left(\frac{z}{W}\right)+\sqrt{\left(\frac{z}{W}\right)^2+1}\right)}{\left(\frac{z}{W}\right)+\sqrt{\left(\frac{z}{W}\right)^2+1-F^2}}\right)\\
&- \left(1-\frac{F}{2}\right)^2\log\left(\frac{\left(\frac{z}{W}\right)^2+1+\left(\frac{z}{W}\right)\sqrt{\left(\frac{z}{W}\right)^2+1-F^2}-F}{(1-F)\sqrt{\left(\frac{z}{W}\right)^2+1}\left(\left(\frac{z}{W}\right)+\sqrt{\left(\frac{z}{W}\right)^2+1}\right)}\right)\\
&\left.- \left(1+\frac{F}{2}\right)^2\log\left(\frac{\left(\frac{z}{W}\right)^2+1+\left(\frac{z}{W}\right)\sqrt{\left(\frac{z}{W}\right)^2+1-F^2}+F}{(1+F)\sqrt{\left(\frac{z}{W}\right)^2+1}\left(\left(\frac{z}{W}\right)+\sqrt{\left(\frac{z}{W}\right)^2+1}\right)}\right)\right],
\end{aligned}
\tag{5}
$$

where $F = I_0/I_c$, $I_c = 2WdJ_c$, and the thickness d of the strip is ignored relative to the width $2W$. Note that the apparent loss is zero when the leads are brought together at the height $z = 0$. The reason for this is that both terms on the right-hand side of Eq. (1) are then zero.

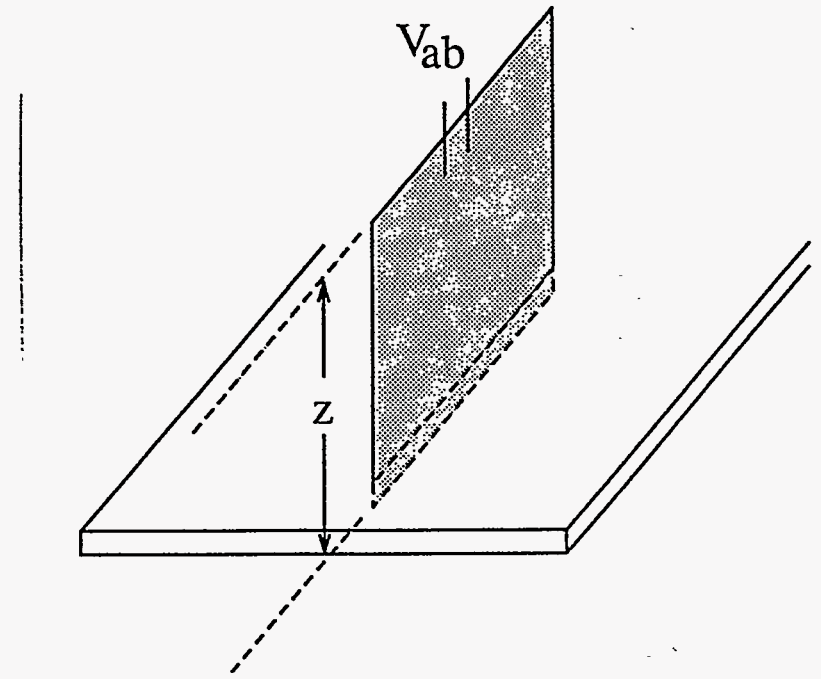

Fig. 2. The perpendicular case: Measuring-circuit leads extend to a height z above the sample.

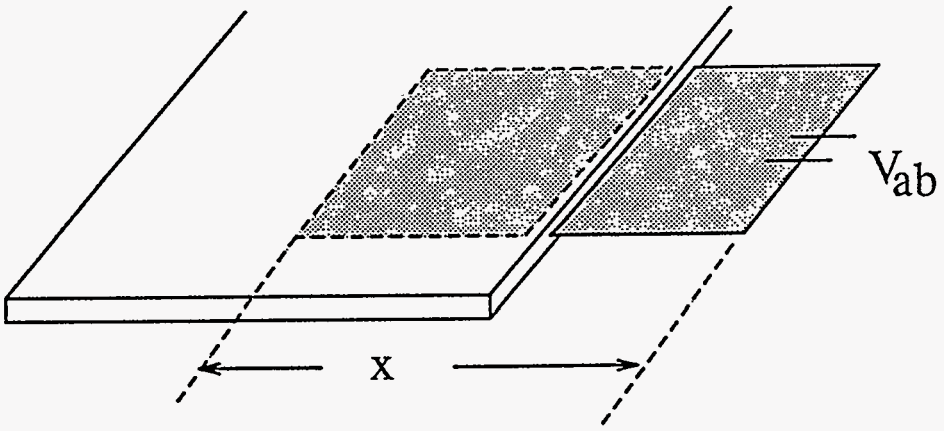

Fig. 3. The parallel case: Measuring-circuit leads extend to the coordinate $x > W$.

Similarly, the apparent loss per cycle per unit length for the strip in the parallel case is

$$L_{\parallel}(F) = \left(\frac{\mu_0 I_c^2}{\pi}\right) \times \left[2\left(\frac{x}{W}\right)\left(\sqrt{\left(\frac{x}{W}\right)^2 - 1 + F^2} - \sqrt{\left(\frac{x}{W}\right)^2 - 1}\right.\right.$$
$$\left.\left. - F\log\left(\frac{\sqrt{\left(\frac{x}{W}\right)^2 - 1}}{\sqrt{\left(\frac{x}{W}\right)^2 - 1 + F^2} - F}\right)\right)$$
$$- \frac{F^2}{2}\log\left(\frac{\sqrt{1-F^2}\left(\left(\frac{x}{W}\right) + \sqrt{\left(\frac{x}{W}\right)^2 - 1}\right)}{\left(\frac{x}{W}\right) + \sqrt{\left(\frac{x}{W}\right)^2 - 1 + F^2}}\right)$$
$$- \left(1 - \frac{F}{2}\right)^2 \log\left(\frac{\left(\frac{x}{W}\right)^2 - 1 + \left(\frac{x}{W}\right)\sqrt{\left(\frac{x}{W}\right)^2 - 1 + F^2} + F}{(1-F)\sqrt{\left(\frac{x}{W}\right)^2 - 1}\left(\left(\frac{x}{W}\right) + \sqrt{\left(\frac{x}{W}\right)^2 - 1}\right)}\right)$$
$$- \left(1 + \frac{F}{2}\right)^2 \log\left(\frac{\left(\frac{x}{W}\right)^2 - 1 + \left(\frac{x}{W}\right)\sqrt{\left(\frac{z}{W}\right)^2 - 1 + F^2} - F}{(1+F)\sqrt{\left(\frac{x}{W}\right)^2 - 1}\left(\left(\frac{x}{W}\right) + \sqrt{\left(\frac{x}{W}\right)^2 - 1}\right)}\right)\Bigg]. \quad (6)$$

Figure 4 shows plots of the apparent loss per cycle per unit length in both the perpendicular and parallel cases for strip geometry versus $F = I_0/I_c$ on a semilogarithmic scale. Shown for comparison is the real (or true loss) per cycle per unit length for strip geometry (solid curve) [8],

$$L_0(F) = \left(\frac{\mu_0 I_c^2}{\pi}\right)\left[(1-F)\log(1-F) + (1+F)\log(1+F) - F^2\right]. \quad (7)$$

Note that $L_0 \propto F^4$ for small $F \ll 1$. We see that the apparent losses $L_\perp$ and $L_\parallel$ agree with L_0 within about 1% when $z/W > 3$ or $x/W > 3$. For large values of z/W and x/W, the following expansions are useful:

$$L_\perp(F) = L_0(F) + \left(\frac{\mu_0 I_c^2}{\pi}\right)\left[-\frac{F^4}{12\left(\frac{z}{W}\right)^2} + \frac{F^4\left(\frac{1}{2} - \frac{F^2}{5}\right)}{8\left(\frac{z}{W}\right)^4} + O\left(\frac{1}{\left(\frac{z}{W}\right)^6}\right)\right], \quad (8)$$

$$L_\parallel(F) = L_0(F) + \left(\frac{\mu_0 I_c^2}{\pi}\right)\left[\frac{F^4}{12\left(\frac{x}{W}\right)^2} + \frac{F^4\left(\frac{1}{2} - \frac{F^2}{5}\right)}{8\left(\frac{x}{W}\right)^4} + O\left(\frac{1}{\left(\frac{x}{W}\right)^6}\right)\right]. \quad (9)$$

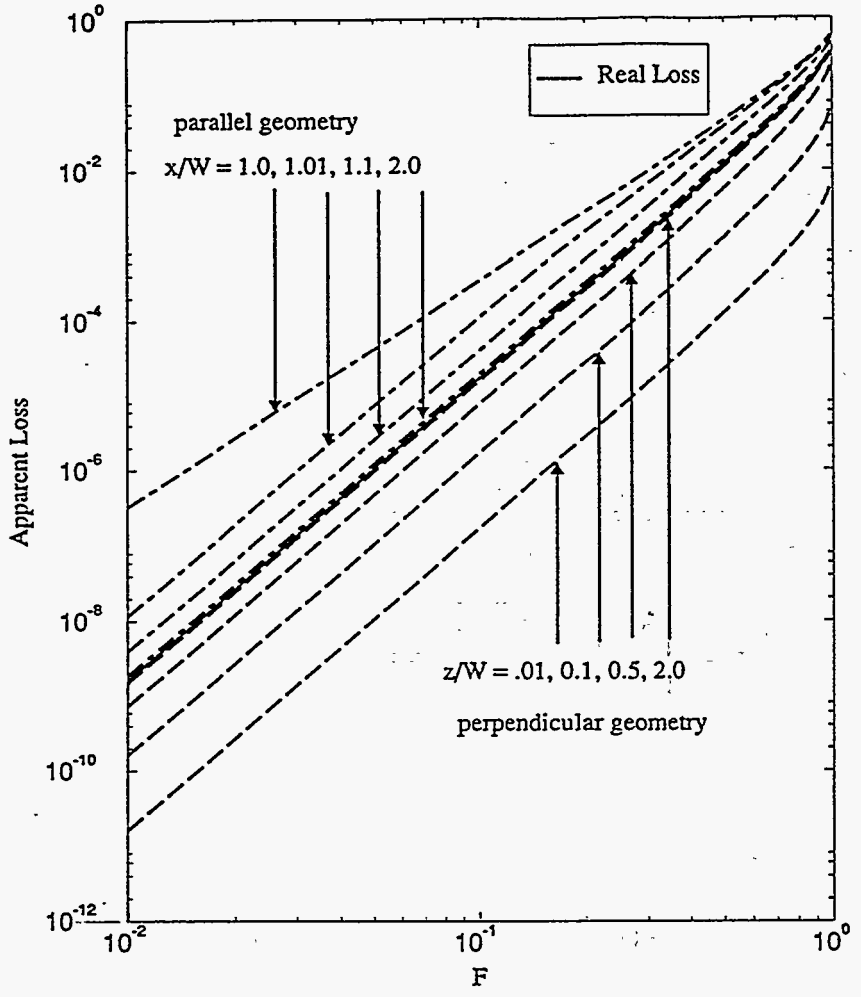

Fig. 4. Apparent loss per cycle per unit length (in units of $\mu_0 I_c^2/\pi$) for a strip of width $2W$ and thickness d, calculated as described in the text for parallel (dot-dashed curves) and perpendicular geometry (dashed curves). The real loss, representing the actual power dissipation made up by the power supply is shown by the solid curve [8].

For samples of elliptical cross section, the apparent loss per cycle per unit length can be calculated by a procedure very similar to that described above, except that the current density and magnetic fields are those found in Ref. [8]. We consider the elliptical cross section to be characterized by a semimajor axis W and semiminor axis $d/2$, such that the width of the sample is $2W$ and the thickness at the thickest point is d. The critical current is thus $I_c = (\pi/2)WdJ_c$,

and the ratio of the semiminor axis to the semimajor axis is $a = d/2W$. The results are, for the perpendicular case,

$$
\begin{aligned}
L_{\perp}(F) = \left(\frac{\mu_0 I_c^2}{\pi}\right) \times & \\
& \left[\frac{2\left(\frac{z}{d}\right)}{3(1-a^2)^2}\left(\left(2\left(\frac{z}{W}\right)^2-(3F-5)(1-a^2)\right)\sqrt{\left(\frac{z}{W}\right)^2+(1-a^2)}\right.\right. \\
& \left.-\left(2\left(\frac{z}{W}\right)^2-(2F-5)(1-a^2)\right)\sqrt{\left(\frac{z}{W}\right)^2+(1-F)(1-a^2)}\right) \\
& -\frac{F^2}{2}\log\left(\frac{\sqrt{1-F}\left(\left(\frac{z}{W}\right)+\sqrt{\left(\frac{z}{W}\right)^2+(1-a^2)}\right)}{\left(\frac{z}{W}\right)+\sqrt{\left(\frac{z}{W}\right)^2+(1-F)(1-a^2)}}\right) \\
& -\left(1-\frac{F}{2}\right)^2\log\left(\frac{\left(\frac{z}{W}\right)-\sqrt{\left(\frac{z}{W}\right)^2+(1-a^2)}}{\left(\frac{z}{W}\right)+\sqrt{\left(\frac{z}{W}\right)^2+(1-a^2)}}\right) \\
& \left.-\left(1-\frac{F}{2}\right)^2\log\left(\frac{\left(\frac{z}{W}\right)+\sqrt{\left(\frac{z}{W}\right)^2+(1-F)(1-a^2)}}{\left(\frac{z}{W}\right)-\sqrt{\left(\frac{z}{W}\right)^2+(1-F)(1-a^2)}}\right)\right]
\end{aligned}
\tag{10}
$$

and, for the parallel case,

$$
\begin{aligned}
L_{\parallel}(F) = \left(\frac{\mu_0 I_c^2}{\pi}\right) \times & \\
& \left[\frac{2\left(\frac{x}{W}\right)}{3(1-a^2)^2}\left(\left(2\left(\frac{x}{W}\right)^2+(3F-5)(1-a^2)\right)\sqrt{\left(\frac{x}{W}\right)^2-(1-a^2)}\right.\right. \\
& \left.-\left(2\left(\frac{x}{W}\right)^2+(2F-5)(1-a^2)\right)\sqrt{\left(\frac{x}{W}\right)^2-(1-F)(1-a^2)}\right) \\
& -\frac{F^2}{2}\log\left(\frac{\sqrt{1-F}\left(\left(\frac{x}{W}\right)+\sqrt{\left(\frac{x}{W}\right)^2-(1-a^2)}\right)}{\left(\frac{x}{W}\right)+\sqrt{\left(\frac{x}{W}\right)^2-(1-F)(1-a^2)}}\right) \\
& -\left(1-\frac{F}{2}\right)^2\log\left(\frac{\left(\frac{x}{W}\right)-\sqrt{\left(\frac{x}{W}\right)^2-(1-a^2)}}{\left(\frac{x}{W}\right)+\sqrt{\left(\frac{x}{W}\right)^2-(1-a^2)}}\right) \\
& \left.-\left(1-\frac{F}{2}\right)^2\log\left(\frac{\left(\frac{x}{W}\right)+\sqrt{\left(\frac{x}{W}\right)^2-(1-F)(1-a^2)}}{\left(\frac{x}{W}\right)-\sqrt{\left(\frac{x}{W}\right)^2-(1-F)(1-a^2)}}\right)\right].
\end{aligned}
\tag{11}
$$

Figure 5 shows plots of the apparent loss per cycle per unit length in both the perpendicular and parallel cases for elliptical cross sections versus $F = I_0/I_c$ on a semilogarithmic scale. Shown for comparison is the real (or true loss) per cycle per unit length for elliptical cross sections (solid curve) [8],

$$L_0(F) = \left(\frac{\mu_0 I_c^2}{\pi}\right)\left[(1-F)\log(1-F) + (2-F)\frac{F}{2}\right]. \tag{12}$$

Note that $L_0 \propto F^3$ for small $F \ll 1$. We find that the apparent losses $L_\perp$ and $L_\parallel$ agree with L_0 within about 1% when $z/W > 3$ or $x/W > 3$. For large values of z/W and x/W, the following expansions for elliptical cross sections are useful:

$$L_\perp(F) = L_0(F) + \left(\frac{\mu_0 I_c^2}{\pi}\right)\left[-\frac{(1-\alpha^2)F^3}{12\left(\frac{z}{W}\right)^2} + \frac{(1-\alpha^2)^2(2-F)F^3}{32\left(\frac{z}{W}\right)^4} + O\left(\frac{1}{\left(\frac{z}{W}\right)^6}\right)\right], \tag{13}$$

$$L_\parallel(F) = L_0(F) + \left(\frac{\mu_0 I_c^2}{\pi}\right)\left[\frac{(1-\alpha^2)F^3}{12\left(\frac{x}{W}\right)^2} + \frac{(1-\alpha^2)^2(2-F)F^3}{32\left(\frac{x}{W}\right)^4} + O\left(\frac{1}{\left(\frac{x}{W}\right)^6}\right)\right]. \tag{14}$$

Note that for both the strip geometry and elliptical cross sections the apparent loss in the parallel geometry is an overestimate of the true loss, but the apparent loss in the perpendicular geometry is an underestimate. The predicted behavior has been confirmed, at least qualitatively by Fleshler et al. [11][12].

The above calculations have been carried out for monolithic type-II superconducting strips of rectangular or elliptical cross section, in which the critical depinning current density is J_c. Our calculations also should apply, with minor modifications, to strip-like composite conductors containing a uniform density (volume fraction f_s) of untwisted superconducting filaments (each filament characterized by J_c) embedded in a normal-metal matrix. It can be shown that application of a current to such a composite conductor induces a current that flows initially with highest density in the filaments near the edge. Only when the current density in the outermost filaments exceeds J_c does current transfer to filaments farther from the edge, thereby permitting magnetic flux to penetrate more deeply into the composite conductor. Under the application of an ac current, the penetration of magnetic flux into composites is thus very similar to that into monolithic superconductors. The maximum supercurrent density, averaged over the composite's total cross section, is the engineering critical current density, $J_e = f_s J_c$. To describe losses of multifilamentary composite conductors using Eqs. (5)-(14), one must therefore replace J_c by $J_e = f_s J_c$ and I_c by $I_c = 2WdJ_e$ for rectangular cross section or $I_c = (\pi/2)WdJ_e$ for elliptical cross section.

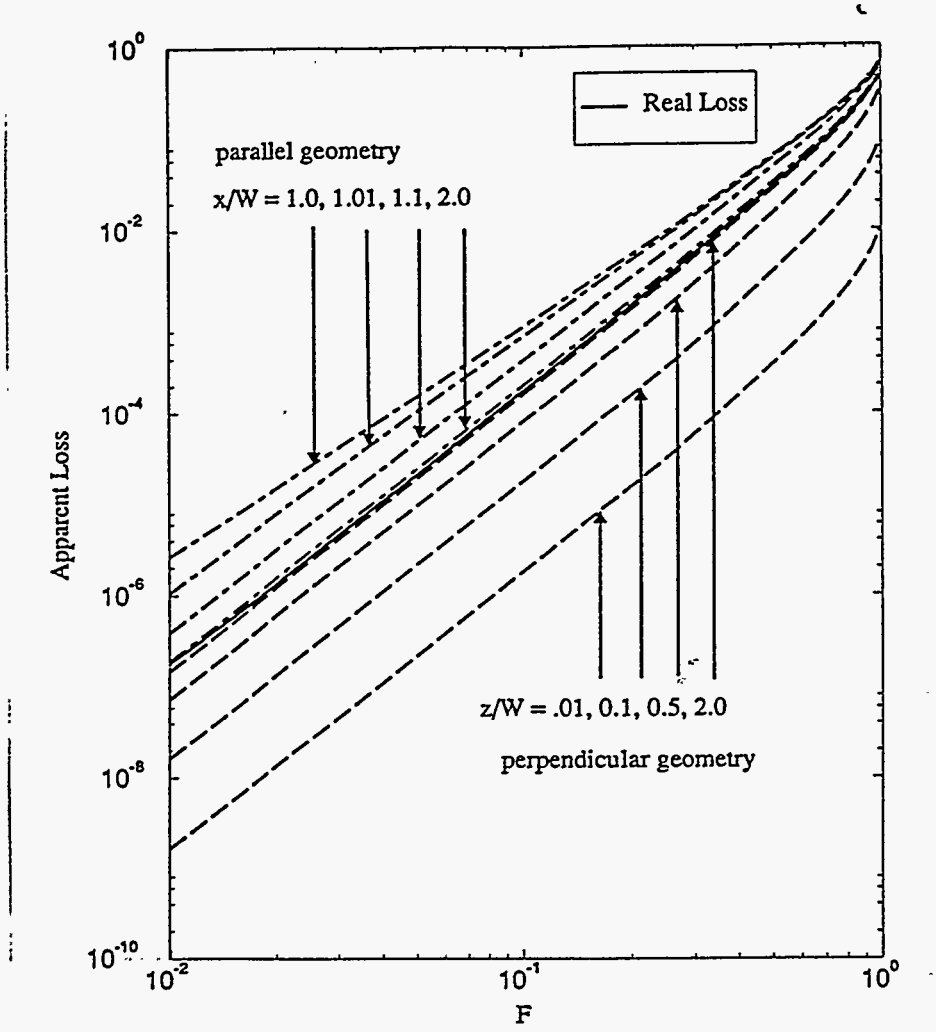

Fig. 5. Apparent loss per cycle per unit length (in units of $\mu_0 I_c^2/\pi$) for a sample of elliptical cross section ($\alpha \to 0$), calculated as described in the text for parallel (dot-dashed curves) and perpendicular geometry (dashed curves). The real loss, representing the actual power dissipation made up by the power supply is shown by the solid curve [8].

3 Summary and Acknowledgments

In this paper we have theoretically studied the hysteretic ac transport losses of type-II superconducting strips of rectangular and elliptical cross section carrying an ac current. Our theory shows that the apparent loss per cycle per unit length

depends both upon the placement of the voltage contacts on the surface of the superconductor and upon the arrangement of the measuring circuit leads as they are brought away from the sample before being twisted and led out to the voltmeter. Our results show that the apparent loss per cycle is underestimated in the perpendicular arrangement sketched in Fig. 2 but is overestimated in the parallel arrangement sketched in Fig. 3. We have presented several expressions that can be used to determine the amount by which the apparent loss per cycle for a given measuring circuit configuration differs from the true loss per cycle.

Ames Laboratory is operated for the U.S. Department of Energy by Iowa State University under Contract No. W-7405- Eng-82. This work was supported by the Director for Energy Research, Office of Basic Energy Sciences. We thank E. Zeldov, V. G. Kogan, M. Benkraouda, A. P. Malozemoff, and S. Fleshler for stimulating discussions and helpful advice.

References

1. M. Ciszek, A. M. Campbell, B. A. Glowacki, Physica C 233, 203 (1994).
2. M. Ciszek, B. A. Glowacki, S. P. Ashworth, A. M. Campbell, and J. E. Evetts, IEEE Trans. Appl. Superconductivity 5, 709 (1995).
3. Y. Yang, T. Hughes, C. Beduz, D. M. Spiller, Z. Yi, and R. G. Scurlock, IEEE Trans. Appl. Superconductivity 5, 701 (1995).
4. A. M. Campbell, IEEE Trans. Appl. Superconductivity 5, 687 (1995).
5. J. R. Clem, Phys. Rev. B 1, 2140 (1970).
6. J. R. Clem, Phys. Reports 75, 1 (1981).
7. J. R. Clem, J. Low Temp. Phys. 42, 363 (1981).
8. W. T. Norris, J. Phys. D 3, 489 (1970).
9. E. H. Brandt and M. Indenbom, Phys. Rev. B 48, 12893 (1993).
10. E. Zeldov, J. R. Clem, M. McElfresh, and M. Darwin, Phys. Rev. B 49, 9802 (1994).
11. S. Fleshler, L. T. Cronis, G. E. Conway, A. P. Malozemoff, T. Pe, J. McDonald, J. R. Clem, G. Vellego, and P. Metra, Appl. Phys. Lett. (1995).
12. A. P. Malozemoff, Q. Li, S. Fleshler, G. Snitchler, and D. Aized, Taiwan International Conference on Superconductivity, Hualien, Taiwan, R.O.C., August 8-11, 1995.

This book was processed by the author using the TEX macro package from Springer-Verlag.